Vortex lattice dynamics in $DyBa_2Cu_3O_7/(Sr_{1-x}Ca_x)RuO_3$ multilayers

L. Miéville,* E. Koller, J.-M. Triscone, M. Decroux, and Ø. Fischer
Département de Physique de la Matière Condensée, University of Geneva, 24 Quai E.-Ansermet, 1211 Geneva 4, Switzerland

E. J. Williams
IBM Research Division, Zürich Research Laboratory, Säumerstrasse 4, 8803 Rüschlikon, Switzerland
(Received 18 March 1996)

We have investigated vortex dynamics in $DyBa_2Cu_3O_7/(Sr_{1-x}Ca_x)RuO_3$ multilayers in parallel and perpendicular applied magnetic fields. In both configurations, we have measured activation energies U for flux motion and determined vortex coupling through either ferromagnetic ($SrRuO_3$) or nonmagnetic ($CaRuO_3$) barriers. Coupled motion of pancake vortices belonging to different $DyBa_2Cu_3O_7$ layers occurs for nonmagnetic barriers ($CaRuO_3$) as large as several hundreds of Å . In the case of ferromagnetic barriers ($SrRuO_3$), 50 Å was found to be sufficient to decouple the vortices between the barrier. The ferromagnetism present in the $SrRuO_3$ barrier is believed to be responsible for such behavior. [S0163-1829(96)03934-3]

I. INTRODUCTION

Vortex dynamics in the mixed state of high-temperature superconductors have been extensively studied since their discovery in 1986.[1] The stacking sequence of their layered crystal structure has been shown to have a direct influence on their highly anisotropic superconducting properties. An original way to address some of the questions related to the importance of anisotropy in high-T_c superconductors consists of modifying this stacking sequence in a controlled manner. For that goal, thin-film growth is a powerful technique which has led to numerous studies involving heterostructures or artificial multilayers consisting of superconducting-nonsuperconducting materials grown epitaxially on different substrates. In most of these investigations, the barrier material was chosen to be structurally close to the superconductor.[2–5] In the case of $YBa_2Cu_3O_7$ (YBCO) based superlattices, different types of barriers such as $PrBa_2Cu_3O_7$ (insulating), $Y_{0.55}Pr_{0.45}Ba_2Cu_3O_7$ (semiconducting), or $Y_{0.6}Pr_{0.4}Ba_2Cu_3O_7$ (superconducting), have ben used.[6–9] However, other material combinations are possible with different types of oxides which still present good structural and chemical compatibility with the superconductor. This allows the combination of materials with very different electronic and magnetic properties.[10–15] In this paper, we present a study of vortex dynamics in superconducting-ferromagnetic heterostructures based on the superconductor $DyBa_2Cu_3O_7$ (DyBCO) and $(Sr_{1-x}Ca_x)RuO_3$ as a barrier material. The $(Sr_{1-x}Ca_x)RuO_3$ (SCRO) perovskite is an ideal system to study the possibility of proximity coupling through a ferromagnetic material. $SrRuO_3$ (SRO) is a metallic perovskite which is ferromagnetic below 160 K (Ref. 16) but $CaRuO_3$ (CRO) does not exhibit any magnetic order at low temperature.[17] In more recent studies, the fabrication of SCRO thin films and YBCO-SCRO-YBCO Josephson junctions have been reported.[18–21] In this paper we have investigated the flux dynamics and the dimensionality of the vortex lattice by examining the vortex coupling between two superconducting layers separated by a SCRO barrier. For that goal, we have deposited two series of multilayers, one with a ferromagnetic barrier (DyBCO/SRO) and another with a nonferromagnetic barrier (DyBCO/CRO). The flux motion has been studied in resistive transitions in magnetic fields. In the tail of the transitions a thermally activated flux motion is observed, as shown previously by Palstra *et al.* in YBCO single crystals.[22] The activation energies U, determined from this thermally activated behavior, are directly related to the anisotropy of the flux-line lattice and hence are sensitive to a possible coupling between the superconducting layers (for thin enough superconducting layers). The possibility of varying the magnetic properties of the barrier allows us to better understand the role of ferromagnetism in the coupling and can bring additional information on the type of mechanism responsible for it. This is the first report of such a study in a high-T_c superconductor based multilayers and superlattices.

II. PREPARATION AND CHARACTERIZATION OF THE SAMPLES

Before growing the heterostructures, we investigated the magnetic properties of single $SrRuO_3$ films by using a superconducting quantum interference device (SQUID). A curie temperature of $\sim$155–160 K was determined from the onset of magnetization and from a kink[23] in the resistivity, in good agreement with the reported values in the literature. The exact structure of SCRO is indeed orthorhombic due to the small size of the Sr^{2+} and Ca^{2+} ions, which creates a small distortion from the cubic structure. Out-of-plane x-ray analyses showed that the growth orientation on (100) $SrTiO_3$ substrates is (110). If we neglect the distortion, we can index the reflections to a pseudocubic lattice with parameters varying continuously from 3.92 Å ($x=0$) to 3.85 Å ($x=1$). These values are close to the DyBCO a-b axes, which should guarantee a good growth quality of the heterostructures. The multilayers have been deposited by on-axis magnetron sputtering in an UHV chamber. Typical deposition parameters for the SCRO are 75 mTorr of Ar and 25 mTorr of O_2 at 680 °C. These conditions were changed to 700 mTorr of Ar and 80 mTorr of O_2 at 780 °C for DyBCO.

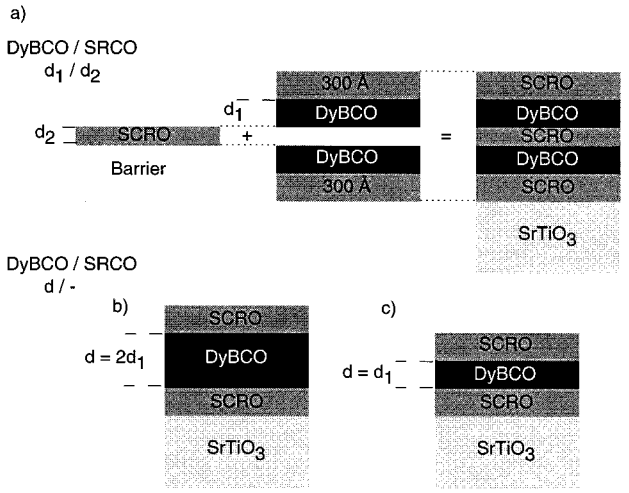

FIG. 1. Schematic diagram of the DyBCO/SCRO (d_1/d_2) multilayers. (a) Two superconducting DyBCO layers of thickness d_1 are separated by a d_2 thick SCRO barrier. 300-Å SCRO buffer and covering layers are also deposited. Limiting cases for no central barrier (b) and an infinite separation (c) are also shown.

More details on the preparation and the characterization can be found elsewhere.[24,25]

The construction of the samples used in this study is illustrated in Fig. 1 and can be described as follows. Two superconducting layers of thickness d_1 of DyBCO are separated by a SCRO barrier of variable thickness d_2. In order to assure an identical environment for the superconducting layers, a buffer layer and a covering layer (300 Å SCRO each) are also deposited [notation d_1/d_2, see Fig. 1(a)]. Figures 1(b) and 1(c) illustrate the two limiting cases used as a reference in this study (notation $d/-$). They correspond, respectively, to a perfect coupling (i.e., $d=2d$, no central barrier) and to a decoupled case ($d=d$, only one superconducting layer).

X-ray diffraction in the Bragg-Brentano geometry has been used for characterization and deposition rate calibration. In DyBCO/SCRO superlattices, the artifical modulation of the structure is responsible for the appearance of satellite peaks. By using different modulations it is possible to determine the thicknesses of the individual layers with a good precision.[25] For single thin films, the finite size of the sample thickness, as compared to the x-ray coherence length (typically several hundreds of Å) gives rise to additional peaks, located around the main reflections. The distance between these peaks allows a precise determination of the thickness and does not require the growth of superlattices in order to calibrate the deposition rates.[26] An alternative way to calibrate the sample thickness with good precision consists of using x-ray grazing angle diffraction. In that case, the reflections from the two interfaces of the film interfere and form oscillations in the x-ray intensity at low angle ($1°<2\theta<5°$). The period of these oscillations is then used to determine the film thickness. Figures 2(a) and 2(b) present a comparison between these two last phenomena for a DyBCO thin film. Figure 2(a) is a θ-2θ x-ray diffractogram around the (001) reflection. Numerous peaks related to the finite-size effect can be observed. In order to allow a precise determination of the film thickness, we use a simple

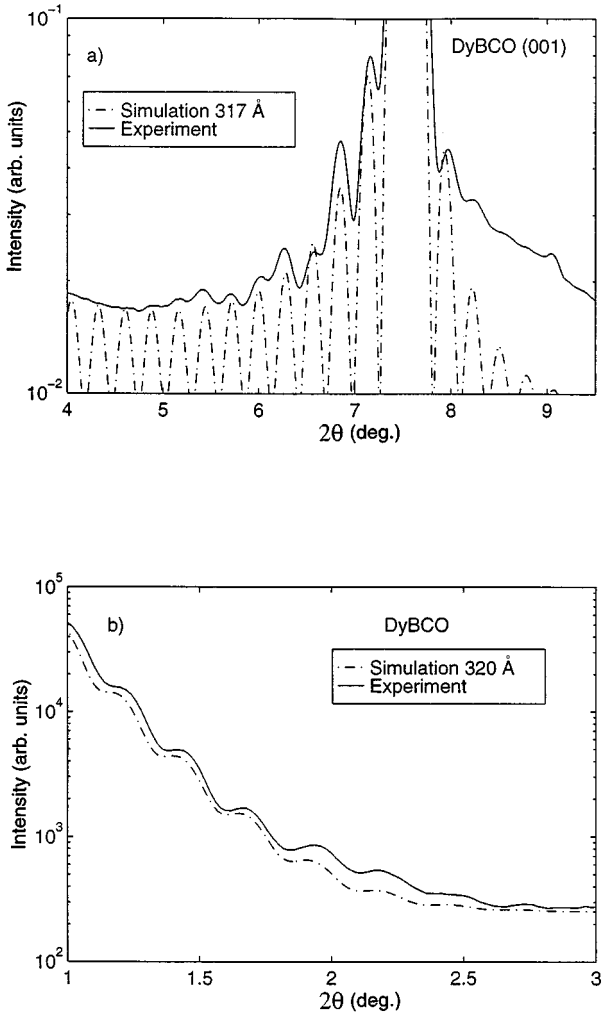

FIG. 2. θ-2θ x-ray diffractograms of a single DyBCO film. (a) Around the (001) reflection. The secondary peaks are due to the finite-size effect. The dashed line is the calculated spectrum, assuming a thickness of $\approx$317 Å . (b) Grazing angle diffraction of the film. The oscillations in the intensity can be fitted to a simple optical model. The calculated spectrum (dashed line) gives a thickness of $\approx$320 Å, in good agreement with the previous result.

model[6,27] to fit the position of these peaks and to extract the thickness of the film. The calculation, assuming a thickness of 317 Å , is shown as a dashed line in Fig. 2(a). The good agreement between the experimental and the calculated positions of the peaks is clearly visible. Note that an exponential factor is used in the calculation to account for the asymmetry present in the oscillations. Figure 2(b) is the grazing angle diffractogram of the same film. Oscillations in the x-ray intensity are observed for small diffraction angles. It should be noted that these oscillations are not to be confused with the finite-size effect peaks described before. Calculations based on a simple optical model.[27,28] allow us to fit the measured spectrum with a very good agreement. The dashed line in Fig. 2(b) represents the calculation, assuming a layer thickness of 320 Å . As one can see in Figs. 2(a) and 2(b), the two methods give similar results for the sample thickness. Such effects could not be observed for SCRO thin films. In that case, we used scanning electron microscopy (SEM) and transmission electron microscopy (TEM) profile

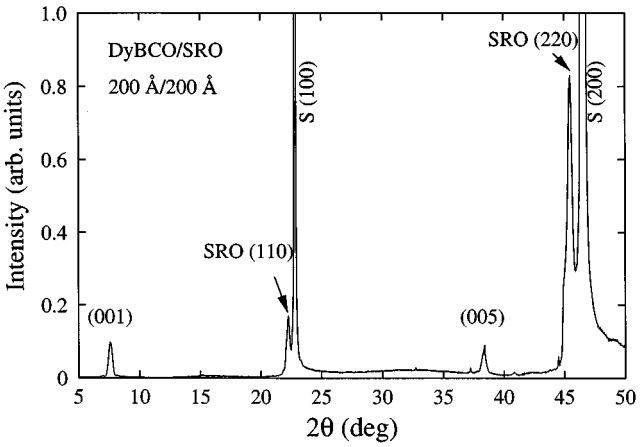

FIG. 3. θ-2θ x-ray diffractogram of a 200 Å /200 Å DyBCO/SRO multilayer.

analyses to determine the deposition rate.

Figure 3 shows a θ-2θ diffractogram of a 200 Å /200 Å DyBCO/SRO multilayer. Only SRO and DyBCO reflections are visible. No trace of extra phases in the heterostructure could be detected. Figure 4 shows a cross-sectional view of a 25 Å SRO barrier surrounded by two 250 Å -thick DyBCO layers (250 Å /25 Å sample). The substrate is visible on the upper-right part of the image. The SRO buffer and covering layers are clearly visible. The two DyBCO layers are easily recognized due to their characteristic layered structure (parallel lines). They are separated by a (25–37) Å -thick SRO barrier. The structure is well defined and the barrier is continuous. Further investigations over larger distances (several thousands of Å) showed no discontinuity of the barrier, confirming the high quality of the structure.

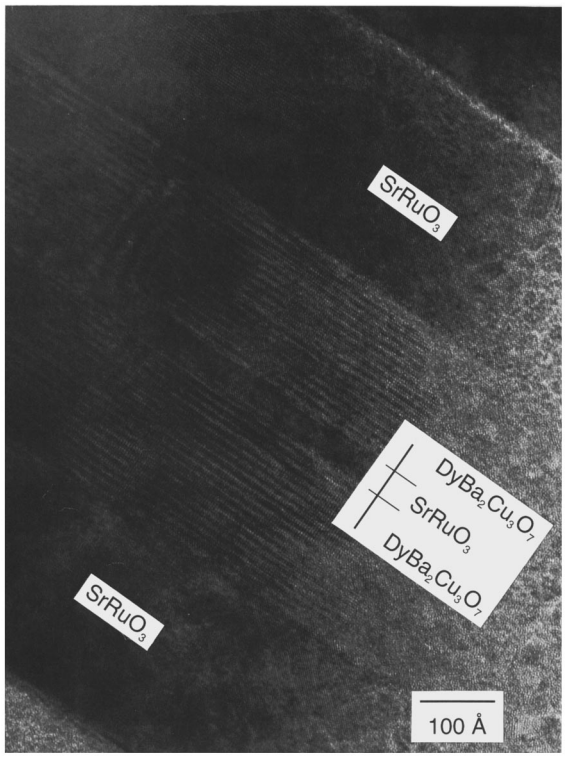

FIG. 4. TEM cross-sectional view of a 200 Å /25 Å DyBCO/SRO multilayer. The substrate is visible in the upper right corner of the image. The barrier thickness is 25–37 Å thick.

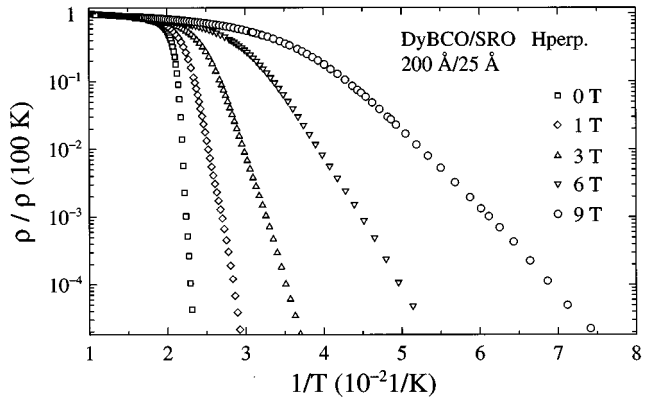

FIG. 5. Normalized resistivity vs $1/T$ for a 200 Å /25 Å DyBCO/SRO multilayer, as a function of perpendicular applied fields.

III. STUDY OF THE VORTEX DYNAMICS IN PERPENDICULAR FIELDS

We have studied the activated behavior of the vortices in applied fields where the I-V characteristics are linear. This activated character can be observed in the tail of the resistive transitions measured by the standard four-points technique. To better illustrate this point, we represent the measured resistivity $\rho(T)$ as a function of applied magnetic field in an Arrhenius plot, i.e., $\ln\rho$ vs $1/T$. Figure 5 shows the normalized resistivity versus temperature and applied magnetic field for a 200 Å /25 Å DyBCO/SRO sample plotted in an Arrhenius graph. The activation energies U are defined as the average slopes of the lower part of the plot. The temperature dependence of U has been previously analyzed[22] and is responsible for some curvature visible on the bottom part of the curves. It has been shown in a previous work[6] that U can nevertheless be used to compare different samples with good precision.

Figure 6 shows the activation energies $\overline{U}$ for different DyBCO/SRO multilayers. The field is applied perpendicular

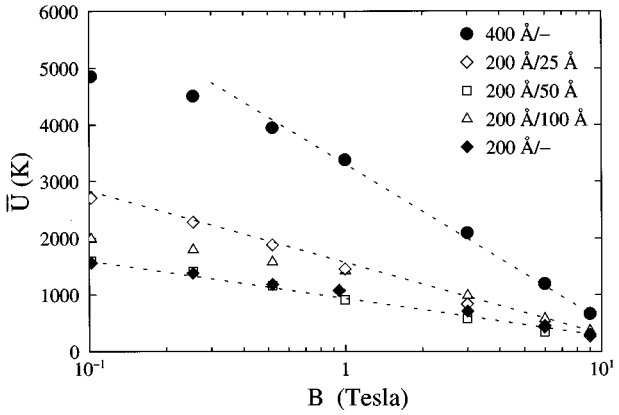

FIG. 6. DyBCO/SRO activation energies $\overline{U}$ as a function of applied perpendicular fields and for different barrier thicknesses. The dashed lines are guides for the eye.

to the CuO_2 planes and to the current passing through the sample. We have measured five multilayers with variable SRO (ferromagnetic) barrier. The activation energy is proportional to the effective thickness involved in the flux jumps up to the limiting correlation length L_c of the vortices.[29] Since this correlation length in DyBCO is close to 400 Å ,[29] which is larger than each DyBCO layer thickness, the presence of coupling between the two superconducting layers should then cause an increase of U as compared to the uncoupled reference sample (200 Å /-). By examining Fig. 6, among the multilayers with a central SRO barrier of 25, 50, or 100 Å , only the activation energy of the 25 Å barrier sample (200 Å /25 Å) exhibits a clear increase (80%) as compared to the uncoupled reference sample (200 Å /-). This is the expected enhancement for strong coupling between the DyBCO layers. However, this result is not in agreement with the (400 Å /-) multilayer corresponding to the reference sample for strong coupling and whose activation energies are surprisingly high in comparison to the uncoupled (200-Å /-) case. We attribute this discrepancy to a relaxation of strain in this multilayer due to the absence of central layer and to the large DyBCO thickness (400 Å). The presence of strain in our multilayers is believed to be the explanation for the observed reduction of the activation energies as compared to those obtained in YBCO/PBCO superlattices with similar YBCO thicknesses.[11,29] For the two others barrier thicknesses (200 Å /50 Å and 200 Å /100 Å samples) no clear sign of coupling is observed. The 100-Å SRO barrier sample shows a slight increase of the activation energy which can be due to strain relaxation but no increase is reported for a thinner barrier of 50 Å .

The magnetic field dependence of the activation energy is logarithmic (see Fig. 6) for all samples, except for the 200 Å/ 100 Å and 400 Å /- samples which show some curvature due to strain relaxation. We can define an effective thickness d_s involved in the motion of the flux and write $U/d_s = -\alpha \ln(B) + \beta$ where α, β are some numerical factors.[29] In the uncoupled reference case, $d_s = 200$ Å , we obtain the numerical values $\alpha = 1.43$ K/Å , and $\beta = 4.68$ K/Å. From that result, we can deduce the effective thickness $d_s \approx 370$ Å related to the increase of the activation energy for the strongly coupled sample (200 Å /25 Å). This value is close to the total DyBCO thickness in the sample, which is the expected result for complete coupling.

Different theoretical explanations have been proposed to account for the ln(B) dependence of the activations energies in perpendicular fields. Following Feigel'man, Geshkenbein, and Larkin,[30] this dependence is indeed related to plastic deformation in the vortex structure. In two dimensions (2D) and because of a short translational correlation length R_c, the free energy to unbind a dislocation pair is finite and leads to an activation energy given by $U = (\phi_0^2 d/16\pi^2 \mu_0 \lambda_{ab}^2) \ln(a_0/\xi_{ab})$ where λ_{ab} and ξ_{ab} are, respectively, the in-plane penetration and coherence lengths, ϕ_0 the flux quantum, d the superconducting thickness, and a_0 the flux-line-lattice spacing. A straightforward calculation assuming the usual DyBCO parameters leads to $\alpha = 3.47$ K/Å , $\beta = 24.2$ K/Å .[29] This is in reasonable agreement with the experimental result for the uncoupled multilayer ($\alpha = 1.43$ K/Å , $\beta = 4.68$ K/Å). Another model, proposed more recently by Jensen *et al.*,[31] presents a different explanation based on the dominant contribution of thermally generated vortex-antivortex pairs. More details of these two models can be found in Refs. 6 and 32.

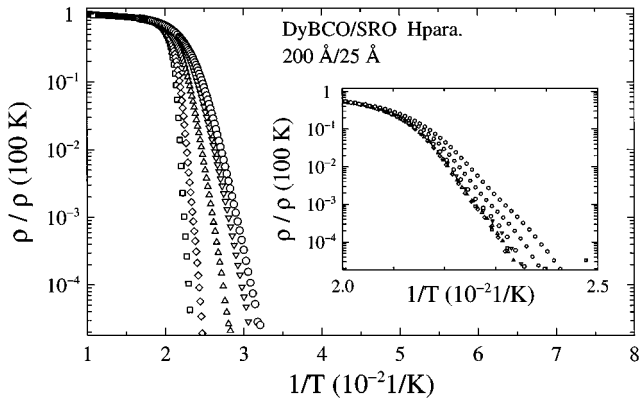

FIG. 7. Arrhenius plot of a 200 Å /25 Å DyBCO/SRO multilayer. The applied fields (0, 1, 3, 6, and 9 T) are parallel to the plane of the film (DyBCO a-b plane). Inset: close views of the 0.01, 0.03, 0.06, 0.15, 0.25, 0.5, and 0.75 T plots.

IV. STUDY OF THE VORTEX DYNAMICS IN PARALLEL FIELDS

In order to further investigate the presence of coupling in our multilayers, we have undertaken a complementary study in a different field configuration, i.e., by applying the magnetic field parallel to the plane of the films and thus to the a-b plane of DyBCO. Figure 7 shows the normalized resistivity versus temperature for a 200 Å /25 Å DyBCO/SRO multilayer in parallel applied fields, plotted in an Arrhenius graph. We observe a reduced broadening of the transition as compared to the measurements done in the perpendicular configuration (see Fig. 5). A striking feature is the absence of any field dependence of the transition below 0.15 T, as it can be seen in the insert of Fig. 7. The activation energies are field independent for sufficiently low applied fields. We can then define a crossover field B^*, above which a field dependent U and a reduction of the activation energies are observed. Figure 8 is a plot of the normalized activation energies for our DyBCO/SRO multilayers as a function of the field applied parallel to the a-b plane of the DyBCO layers. The vertical scale has been changed for each sample in order to highlight the value of the crossover field B^*, indicated by arrows. We clearly observe a plateau in the activation energies below B^*, followed by a decrease of U for $B > B^*$. The presence of this plateau is believed to be due to remanent field from the external coil or to thermally generated pairs in the direction perpendicular to the applied field.[33] The unsensitivity of U on the magnetic field when $B < B^*$ shows that it is energetically unfavorable for the vortices to penetrate the superconductor when a small field is applied parallel to the multilayers. In the case of thin decoupled layers, we can describe this situation by calculating the lower critical field B_{c1} as a function of the thicknessof the layers.[34,35] We obtain $B_{c1}(0) = [2\lambda_{ab}(0)\phi_0 / \pi\lambda_c(0)d^2] \ln[d/\xi_{\text{eff}}(0)]$ where λ_c, λ_{ab} are the c and ab penetration depths, respectively; ϕ_0 is the flux quantum; d is the superconducting thickness;

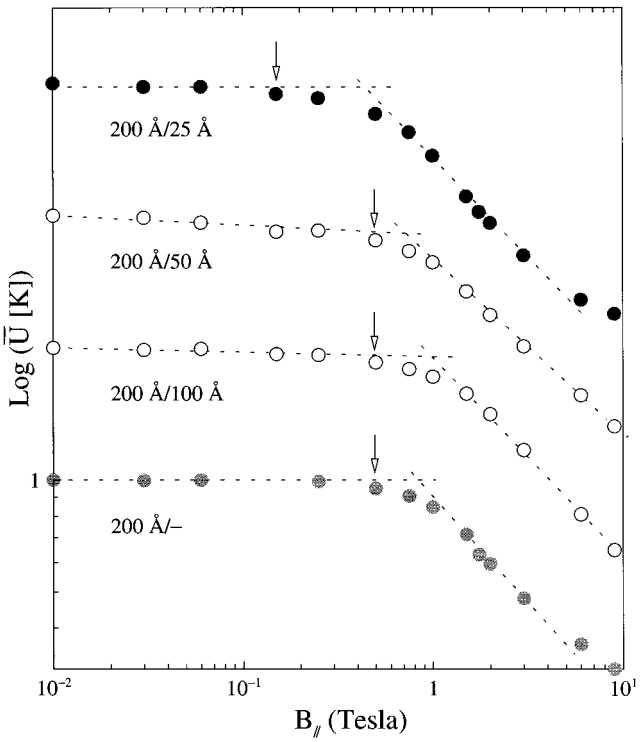

FIG. 8. Normalized DyBCO/SRO activation energies $\overline{U}$ as a function of fields applied parallel to the plane of the film and for different barrier thicknesses. The dashed lines provide a guide for the eye.

and $\xi_{\mathrm{eff}}=\sqrt{\xi_{ab}\xi_c}$ the effective superconducting coherence length. As a first order of approximation, we can write this expression as $B_{c1}d^2\approx$const.

In order to test this prediction, we grew single uncoupled DyBCO films surrounded by SRO. This way, we could compare the B^* dependence on the thickness of the superconducting layer with the predicted value given by the above formula. Figure 9 shows the activation energies as a function of the applied parallel fields, for different DyBCO thicknesses. The arrows indicate a d^2 dependence of B^*, as given

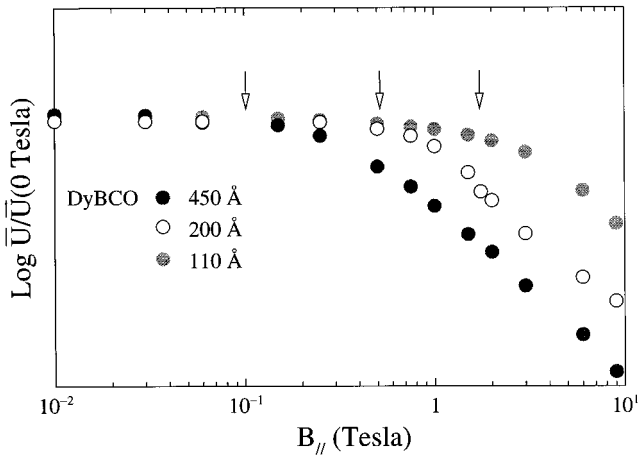

FIG. 9. Normalized SRO-DyBCO-SRO trilayers activation energies U as a function of applied fields parallel to the plane of the film and for different DyBCO thicknesses.

in the first-order approximation of the formula. The agreement is reasonable with the measured B^* values. An exact calculation for a 450 Å thin film, assuming the usual parameters for DyBCO, gives $B_{c1}\approx 0.66$ T, to be compared with the experimental result $B^*\approx 0.1$ T. Since the activation energies are measured near T_c, the relevant penetration depth and coherence length should be extrapolated from zero temperature to near T_c, which should reduce the predicted B_{c1} value. A further confirmation of the formula is also illustrated by the very large (>20 T) B^* observed in YBCO/PBCO multilayers for 24 Å decoupled YBCO.[34]

More interestingly, a change in the B^* value is reported for the 200 Å /25 Å sample, as compared to the other multilayers. It is reasonable to assume that the reduction of B^*, observed in the 200 Å /25 Å multilayer, is due to the presence of coupling, as described previously in the perpendicular analysis (see also Ref. 33). A tempting way to calculate the increase in the effective thickness due to this coupling would be to use the $B^*d^2=$const approximation. Taking $d=200$ Å , $B^*=0.5$ T (200 Å /- sample, see Fig. 7), we deduce an effective thickness of $d\approx 365$ Å for the 200 Å /25 Å sample ($B^*=0.15$ T). This result is indeed in good agreement with the effective thickness $d_s\approx 370$ Å obtained in the perpendicular analysis. However, the validity of the approximation used for decoupled DyBCO layer is still unclear for coupled systems and a quantitative analysis remains questionable. It should also be noted that the parallel analysis is based on the variation of the activation energy and not on its absolute value as for the perpendicular configuration. In the latter case, some possible degradation in our samples an cause some fluctuation in the absolute measure of U. An example of such degradation is visible in the inset of the Fig. 7 where the repeated thermic cycles lead to a slight change in the slope of the Arrhenius curves for $\rho/\rho(100\ \mathrm{K})<10^{-3}$. Such a problem can lead to a difficult interpretation in the perpendicular case. However, in the parallel analysis, the relative variation of U is not affected and the determination of B^* enables a more precise measure of the coupling. This is illustrated in Fig. 8 where no change in the B^* value is reported for the 50 Å and the 100 Å barrier, as compared to the reference sample (200 Å/-). This confirms that 50 Å of SRO is sufficient to decouple the vortices. Such a conclusion cannot be drawn from the perpendicular analysis.

In order to determine the effect of a nonmagnetic barrier on the coupling of the vortices, we have grown a series of multilayers with different CRO barrier thicknesses. Figure 10 presents the activation energies of these multilayers as a function of the applied parallel fields for nonferromagnetic CRO barriers 100 and 300 Å thick. The reference for a decoupled system is also shown (300 Å /-). The vertical scale has been shifted for each sample in order to exhibit the values of the crossover field B^*, indicated by arrows. This value is reduced for the two barriers, as compared to the uncoupled reference. We conclude from that result that a coupling is observed for barrier thicknesses as large as several hundreds of Å , when the barrier is nonferromagnetic.

A very clear dependence of the coupling on the type of barrier is then reported. In DyBCO/SRO multilayers, 50 Å of SRO between the superconducting DyBCO layers is sufficient to decouple the vortices. In the DyBCO/CRO multilay-

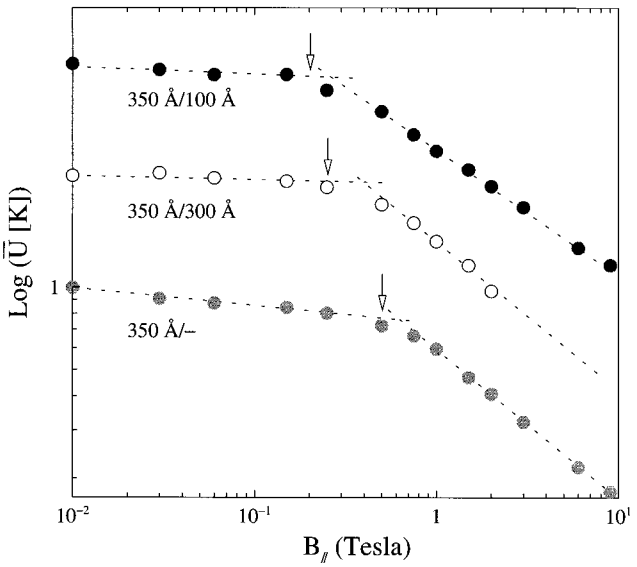

FIG. 10. Normalized DyBCO/CRO activation energies $\overline{U}$ as a function of fields applied parallel to the plane of the film and for different barrier thicknesses. The dashed lines are guides for the eye.

ers, we observe a coupling even for CRO thicknesses as large as several hundreds of Å . This striking difference can be explained by the presence of the ferromagnetic order in the SRO barrier. This is the central result of this work. An interesting comparison can be drawn from similar analyses made on DyBCO/$Y_{0.6}Pr_{0.4}Ba_2Cu_3O_7$ superlattices where a coupling up to several hundreds of Å of metallic barrier has been observed.[6] However, if an insulating PBCO barrier is used, 48 Å are sufficient to decouple the vortices.[29] Recently, a related work on YBCO/$La_{0.67}Ba_{0.33}MnO_3$ superlattices, reported a decoupling length of 46 Å of the LaBaMnO ferromagnetic barrier.[14] For such small barrier thicknesses, the presence of ferromagnetic order becomes questionable.[36] Due to the SRO buffer and covering layers in the DyBCO/SRO multilayers, it has not been possible to measure directly the magnetism of the barrier. It should nevertheless be noted that a 30 Å SRO single film has been shown to be ferromagnetic below 150 K.[37]

V. CONCLUSION

In conclusion, we have measured the activation energies for two series of DyBCO/SCRO multilayers in fields parallel and perpendicular to the *a-b* plane. We find a very distinct behavior for the coupled motion of pancake vortices belonging to the DyBCO layers, depending on the type of barrier we used. In DyBCO/SRO multilayers, 50 Å of SRO between the superconducting DyBCO layers is sufficient to decouple the vortices. In the case of the DyBCO/CRO system, we observe a coupling for CRO thicknesses as large as several hundreds of Å . The presence of ferromagnetism in the SRO barrier is a natural explanation for this striking difference. The measure of the activation energy in parallel fields has proven to be a complementary tool to determine the occurrence of coupling in our multilayers.

ACKNOWLEDGMENTS

We would like to thank L. Antognazza for fruitful and stimulating discussion, and G. Bosch for efficient technical support. This work was supported by the Swiss National Science Foundation.

*Present address: E. L. Ginzton Laboratory Stanford University, Stanford, CA 94305-4085.

[1] J. G. Bednorz and K. A. Muller, Z. Phys. B **64**, 189 (1986).
[2] J.-M. Triscone, Ø. Fischer, O. Brunner, L. Antognazza, A. D. Kent, and M. G. Karkut, Phys. Rev. Lett. **64**, 804 (1990).
[3] Q. Li, X. X. Xi, X. D. Wu, A. Inam, S. Vadlamannati, W. L. McLean, T. Venkatesan, R. Ramesh, D. M. Hwang, J. A. Martinez, and L. Nazar, Phys. Rev. Lett. **64**, 3086 (1990).
[4] Z. Z. Li, H. Rifi, A. Vaurès, S. Megtert, and H. Raffy, Phys. Rev. Lett. **69**, 21 713 (1994).
[5] H. Tabata, T. Kawai, and S. Kawai, Phys. Rev. Lett. **70**, 2633 (1993).
[6] J.-M. Triscone, P. Fivat, M. Andersson, M. Decroux, and Ø. Fischer, Phys. Rev. B **50**, 1229 (1994).
[7] Q. Li, C. Kwon, X. X. Xi, S. Bhattacharya, A. Walkenhorst, T. Venkatesan, S. J. Hagen, W. Jiang, and R. L. Greene, Phys. Rev. Lett. **69**, 21 713 (1992).
[8] D. P. Norton, D. H. Lowndes, S. J. Pennycock, and J. D. Budai, Phys. Rev. Lett. **67**, 1358 (1991).
[9] G. Jakob, P. Przslupski, C. Stolzel, C. Tomé-Rosa, A. Walkenhosrt, M. Schmitt, and H. Adrian, Appl. Phys. Lett. **59**, 1626 (1991).
[10] A. Gupta, R. Gross, E. Olsson, A. Segmuller, G. Koren, and C. C. Tsuei, Phys. Rev. Lett. **64**, 3191 (1990).
[11] U. Baier, R. Fischer, A. Beck, D. Koelle, K.-L. Blocher, L. Alff, and R. Gross, Phys. Rev. B **46**, 11 236 (1992).
[12] K. Horiuchi, T. Kawai, S. Kawai, Y. Fujiwara, and S. Hirotsu, Physica C **209**, 531 (1993).
[13] J. P. Contour, D. Ravelosona, C. Sant, C. Frétigny, C. Dolin, J. Rioux, P. Auvray, and J. Caulet, J. Cryst. Growth **141**, 141 (1994).
[14] G. Jakob, V. V. Moshchalkov, and Y. Bruynseraede, Appl. Phys. Lett. **66**, 2564 (1995).
[15] M. W. Denhoff, P. D. Grant, and J. P. McCaffrey, Can. J. Phys. **70**, 1124 (1992).
[16] J. J. Randall and R. Ward, J. Am. Chem. Soc. **81**, 2629 (1959).
[17] A. Kanbayasi, J. Phys. Soc. Jpn. **44**, 108 (1978).
[18] C. B. Eom, R. J. Cava, R. M. Fleming, J. M. Phillips, R. B. v. Dover, J. H. Marshall, J. W. P. Hus, J. J. Krajewski, and W. F. Peck, Jr., Science **258**, 1766 (1992).
[19] K. Char, L. Antognazza, and T. H. Geballe, Appl. Phys. Lett. **63**, 2420 (1993).
[20] L. Antognazza, K. Char, T. H. Geblle, L. L. H. King, and A. W. Sleight, Appl. Phys. Lett. **63**, 1005 (1993).
[21] R. Domel, C. L. Lia, C. Copetti, G. Ockenfuss, and A. I. Braginski, Supercond. Sci. Technol. **7**, 277 (1994).
[22] T. T. M. Palstra, B. Batlogg, R. B. v. Dover, L. F. Schneemeyer, and J. V. Waszczak, Phys. Rev. B **41**, 6621 (1990).
[23] S. V. Vonsovskii, *Magnetism* (Wiley, New York, 1974), Vol. II, p. 1119.
[24] L. Miéville, E. Koller, J.-M. Triscone, and Ø. Fischer, Physica C **235-240**, 725 (1994).

[25] L. Miéville, E. Koller, J.-M. Triscone, and Ø. Fischer (unpublished).
[26] O. Nakamura, E. Fullerton, J. Guimpel, and I. K. Schuller, Appl. Phys. Lett. **60**, 120 (1992).
[27] L. Miéville, Ph.D. thesis, University of Geneva, 1995.
[28] L. G. Parratt, Phys. Rev. **95**, 359 (1954).
[29] O. Brunner, L. Antognazza, J. M. Triscone, L. Miéville, and Ø. Fischer, Phys. Rev. Lett. **67**, 1354 (1990).
[30] M. V. Feigel'man, V. B. Geshkenbein, and A. I. Larkin, Physica C **167**, 177 (1990).
[31] H. J. Jensen, P. Minnhagen, E. Sonnin, and H. Weber, Europhys. Lett. **20**, 463 (1992).
[32] Y. Suzuki, J.-M. Triscone, M. R. Beasley, and T. H. Geballe, Phys. Rev. B **52**, 6858 (1995).
[33] P. Fivat, J.-M. Triscone, M. Andersson, M. Decroux, and Ø. Fischer, in *Superconducting Superlattices and Multilayers*, edited by I. Bozovic, SPIE Proc. Vol. 2157 (SPIE, Bellingham, WA, 1994), p. 192.
[34] J.-M. Triscone, L. Antognazza, O. Brunner, L. Miéville, M. G. Karkut, P. v. d. Linden, J. A. A. J. Perenboom, and Ø. Fischer, Physica C **185-189**, 210 (1991).
[35] T. P. Orlando and K. A. Delin, *Foundations of Applied Superconductivity* (Addison-Wesley, Reading, MA, 1991), p. 388.
[36] *Magnetism*, edited by G. T. Rado and H. Suhl (Academic, New York, 1963), Vol. III.
[37] C. Ahn (unpublished).